ASPECTS OF THE DETECTION OF SCENE CONGRUENCE*

Martin A. Fischler
Lockheed Palo Alto Research Laboratory
Palo Alto, California 94304

ABSTRACT

The problem of matching two scenes, one contained in the other, arises in many practical picture processing tasks including stereocompilation, classification of photographic data, and map matching for navigation and guidance. Because the images are not exact replicas, but rather noisy and perhaps geometrically distorted versions of the original scenes, it is necessary to develop a body of theory capable of providing answers to questions concerning effects of various types of error, and means for minimizing the effects of such errors. This paper presents a "decision space" approach to the problem for dealing with small amounts of noise and distortion, and a promising new technique for dealing with "rubber sheet" distortion.

INTRODUCTION

Assume we are given images of two scenes, one scene contained in the other, and we wish to determine where the contained scene appears (i.e., has a best match)in the containing scene. We further assume that the images are not exact replicas of either of the scenes, but rather noisy and perhaps geometrically distorted versions of each. The solution to this problem (the detection of scene congruence) has applications in many practical picture processing tasks including stereocompilation, classification of photographic data, terrain change detection, map matching for navigation and guidance, etc.

In many of these tasks it is possible to assume that the noise and distortion processes result in relatively small random differences between the contained and containing scenes. Under these conditions, it is both possible and desirable to employ mathematical techniques in contrast to the heuristic approach currently used for general scene analysis. [Reference (1) is a recent survey which considers much of the general scene analysis work.) This allows the formulation of a comprehensive mathematical model which can provide the insight needed to estimate system performance for different proposed configurations. In particular, such a model must address itself to the generic noise and distortion processes peculiar to scene imaging devices, and characterize the effects of simplifications and uncertainties which will necessarily be inherent in any practical system.

This paper is a summary of Fischler (2) and is concerned with the development of a body of theory needed to implement (especially using digital techniques) practical systems for tasks given above. It considers such questions as: [1] What is the nature of optimal decision procedures for the detection of scene congruence under fairly general noise assumptions?, [2] How do error processes, such as scale change, rotation error, sensor amplitude gain and bias variations, etc., affect system performance, and how can the effects of these errors be minimized without paying an excessive cost penalty?, [3) How do various scene properties or characteristics influence system accuracy?, and [4) What procedures are available for situations in which the small error model is not realistic ?

In any practical situation, the instruments used to view, process, and store scene information have finite resolution or bandwidth. Therefore, invoking the Shannon Sampling Theorem, we can restrict our attention to scenes which can be characterized by a finite array of bounded integers, each integer representing the sensed scene attribute (such as light intensity for a photographic sensor, or radiometric temperature if we are employing an infrared sensor, etc.) at some specified geometric location in the given scene. Questions concerning the analog-digital interface are discussed in Fischler (2) but will be omitted from this summary.

The framework for much of the analysis presented in this paper is established by considering each match location in the containing scene (a point of potential match between the containing and contained scenes) as being associated with a distinct class. The "ideal" representative of each class is the fixed size segment of the containing scene centered at the corresponding match location. The containing scene is called the reference map (RM), and the contained scene is called the sensed map (SM). Any given SM is now assumed to be some (ideal) RM segment which has been perturbed by a specified set of noise and distortion proccesses. Match point determination is thus reduced to a classification task. (See Fig. 1.)

Each map, represented by a collection of N discrete numbers, is considered to be a point in a "signal space" of N-dimensions. Using decision theory concepts [see Refs. (3) through (12)], we show that satisfying a minimum error criterion for match point determination corresponds to measuring some weighted distance function between the signal space image of the SM and each of the RM segments.

To present results having the greatest degree of generality and intuitive appeal, geometric arguments form the basis for most of the development presented here. These geometric arguments are supported by a parallel algebraic development given in Fischler (2).

After developing the decision theoretic model, we consider the effect of scale and rotation error (due to uncertainties in sensor position and orientation) on our decision metric. This analysis is followed by a discussion of amplitude gain and bias errors, i.e., linear transformations of the resolution element values which might be introduced by changes in the medium between the scene and the sensor, or by variations in the sensing system itself. In particular, we consider how the effects of these errors can be eliminated (through "normalization") without specifically detecting their

*Work sponsored by the Lockheed Independent Research Program.

x_1	x_2
1.0	2.3

1 × 2 Sensed Map (SM)

3.5	1.0	1.0
2.0	4.2	4.0

2 × 3 Reference Map (RM)

a. Example of a Sensed Map and Reference Map

	x_1	x_2
RM(A) =	3.5	1.0
RM(B) =	2.0	4.2
RM(C) =	1.0	1.0
RM(D) =	4.2	4.0

b. All Possible 1 × 2 RM Segments in the Reference Map

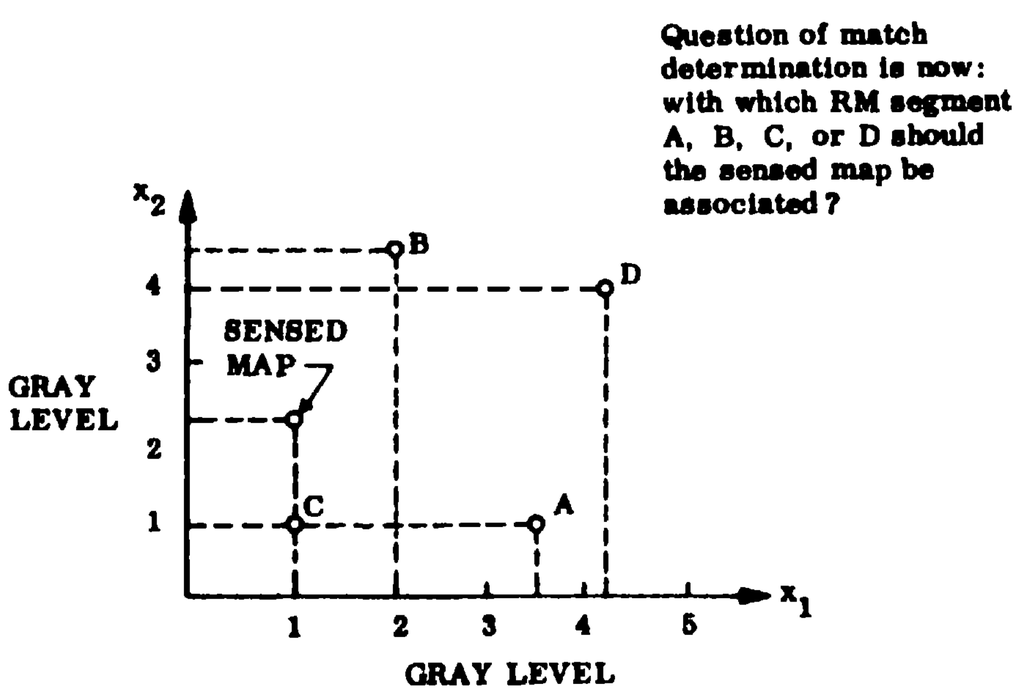

c. RM Segments and Sensed Map Depicted in Signal Space

Fig. 1 Formulation of the Scene Congruence Problem as a Classification Problem With Its Associated Signal Space Representation

presence. The viewpoint of minimizing error effects, rather than detecting and correcting for them, is related to system cost considerations.

The question of remote error (RE) is considered next. RE is defined as the occurrence of two or more RM segments which are essentially identical to the SM, bu are (typically) separated by some nontrivial physical distance in the RM. The relation of probability of RE to such physical quantities as signal-to-noise ratio an< map spatial frequency spectrum is developed. It is also shown that normalization increases the probabilifr of RE.

In many applications, especially those concerned with scene matching for guidance and navigation, the RM (and possibly the SM) may be freely chosen. A discus sion of the factors affecting this choice is given, together with some supporting experimental data.

The final section of this paper is concerned with the question of extreme distortion. In spite of their apparent generality, unaugmented statistical decision theory techniques are useful only in situations where error and distortion processes are held under reasonably tight control. When this is not the case, a different approach to decision making is required. A new, efficient, algorithmic technique for locating one scene in another is presented for cases of extreme distortion. This algorithm is an important development in that it has a computation time requirement which grows linearly with map size, even though it performs a combinatorial search for a best fit using a decomposed SM. For intermediate distortion problems, a simpler technique also involving SM decomposition is shown to be an effective solution.

DECISION PROCEDURES, NOISE PROCESSES, AND SCENE CHARACTERIZATION

As noted in the introduction, this section will first establish a decision theoretic model for match point determination; it then considers the effects of various noise and distortion mechanisms on the decision process, as well as the significance and consequences of normalization. A scene characterization technique based on expressions devised for expected error is offered together with some supporting experimental data.

Since this paper is actually a contracted version of Fischler (2), figure and equation numbers from the original version will be retained where possible to facilitate cross-reference. One effect of this convention will be the omission of figure numbers 2, 3, and 8. References to appendices refer to the original paper although abbreviated appendix material is included where deemed necessary for comprehension.

A Decision Theoretic Model for Match Point Determination

Let the vector $X = (x_1, X_2, . , xN)$ designate the SM. Associated with the ith possible digital match location in the RM is a SM-sized subset of the RM which we designate as

$$RM(i) = Y_i = (y_{i1}, y_{i2}, \ldots, y_{iN}), \qquad 1 \le i \le R$$

Thus (see Fig. 1) the RM is decomposed into a set of R "N-tuples" (i.e., vectors with N components). The SM is a single N-tuple, which we assume is one of the RM(i) which has been perturbed by a specified set of noise and distortion processes.

We would now like to assign X (the SM) to some RM(i) according to a scheme which will minimize the resultant probability of error. That is, we will use a minimum error criterion.

To minimize error, we must assign X to that RM(i) such that Pr[Yf|X] is maximized. The Bayes rule for computing the a posteriori probability is

$$Pr[Y_i|X] = \frac{Pr[X|Y_i]\,Pr[Y_i]}{Pr[X]}$$

If we assume that all Y_i are equally likely to occur (i.e., the SM is equally likely to have been derived from any location in the RM), then we have:

$$\max_i \Pr[Y_i|X] = \max_i \Pr[X|Y_i]$$

Our decision procedure then consists of evaluating $Pr[X|Y_i]$ for all values of i $(1 \leq i \leq R)$ and assigning X to that RM(i) for which Pr|X|Yi) is maximum.

To obtain results having the greatest degree of generality, and still leave our reasoning open to intuitive appraisal, we will employ geometric analysis in a suitably defined "signal space." Appendix B contains a parallel algebraic development which will be used to verify geometrically derived conclusions, and give some insight into the form of the "expected error" expressions under more specific noise assumptions.

Let us consider an N-dimensional Euclidean Hyperspace (EN) in which each of the N coordinate axes corresponds to one of the N components of a vector representing a RM(i) or SM. Thus, any given map will be represented by a single point in EN. Figure 1 illustrates this concept for the case of E^2 and five arbitrarily contrived maps.

A number of observations can be made about "distance" in signal space (see Appendix A). Given points $Y_i = (y_{i1} . y_{i2}. . . . .y_{iN})$ AND Yj Euclidean distance between them is d_{ij} , where:

$$d(i,j) = d_{ij} = \left[\sum_{k=1}^{N} (y_{ik} - y_{jk})^2\right]^{1/2} \qquad [1]$$

The quantity

$$\sum_{k=1}^{N} y_{ik}^2$$

will be called the energy of RM(i), and in Appendix A the justification for this designation is given. Thus, the square of the distance of a point *Yi* [representing RM(i)) from the origin is equal to its "energy" and proportional to its average power. All RM(i) with average power less than or equal to d_2/N lie within the circle centered at the origin with radius d . Similarly, a RM(i) disturbed by additive noise with average power $\mathbf{d_n^2/N}$ would lie somewhere on a circle of radius d_n centered at Yi . In the absence of any special knowledge or assumptions about noise favoring one cell of a RM(i) over another, or one RM(i) over another, it is reasonable to assume that the noise affects each y_{ik}. equally and independently for all (i,k) ; that the noisenas zero mean value; and that the probability of a specific disturbance is inversely related to the magnitude or power associated with the disturbance. That is, the noise is spherically symmetric with the same noise power for all map elements. This situation is illustrated (for N = 2) in Fig. 4a. The equiprobability contours of a noise-disturbed signal,

Distance Metric for Optimal Decision $= \min_i \left[\sum_{j=1}^{N} (x_j - \mu_{ij})^2\right]$

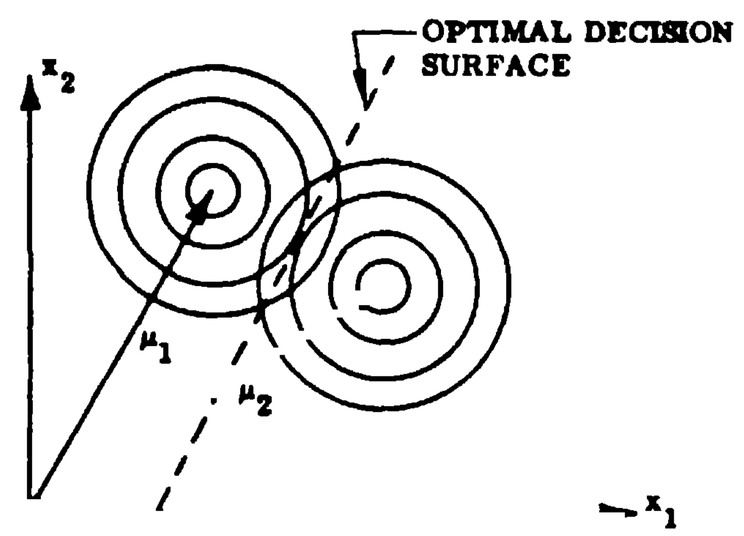

a Case of Spherically Symmetric Noise Which Is Identical and Uncorrelated for All Variables ($\sigma_i = \sigma_j$; $\rho_{ij} = 0$)

Distance Metric for Optimal Decision $= \min_i \left[\sum_{j=1}^{N} \left(\frac{x_j}{\sigma_j} - \frac{\mu_{ij}}{\sigma_j}\right)^2\right]$

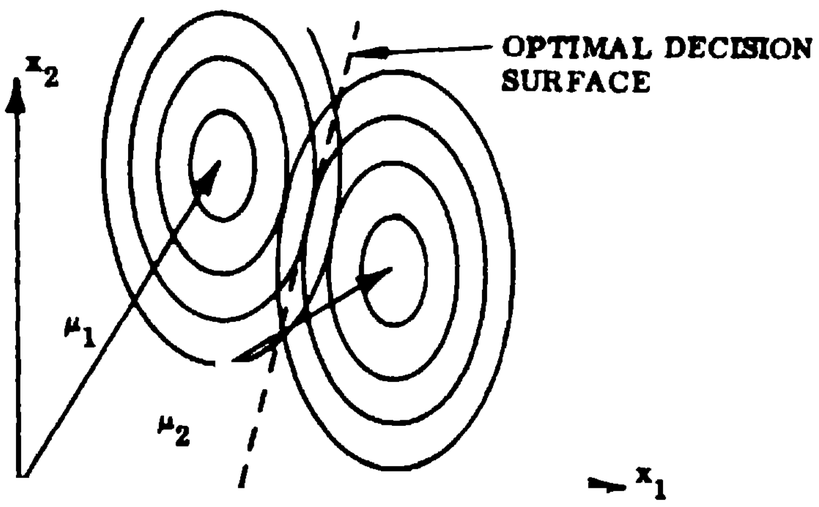

b. Case of Ellipsoidally Symmetric Noise Which Is Not Identical but Is Uncorrelated for All Variables ($\sigma_i \neq \sigma_j$; $\rho_{ij} = 0$)

Distance Metric for Optimal Decision $= \min_i \left[\sum_j \sum_k \tau_{jk} (x_j - \mu_{ij})(x_k - \mu_{ik})\right]$

SUFFICIENT CONDITIONS FOR A LINEAR DECISION SURFACE:
ELLIPSOIDALLY SYMMETRIC
MONOTONICALLY DECREASING
EQUAL COVARIANCE MATRICES

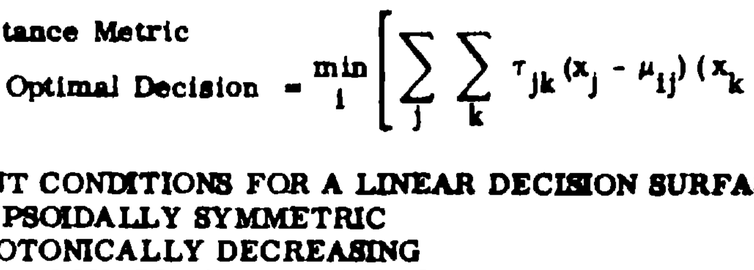

c. Case of Ellipsoidally Symmetric Noise Which Is Not Identical and May Be Correlated for All Variables ($\sigma_i \neq \sigma_j$; $\rho_{ij} \neq 0$)

Fig. 4 Probability Contours and Decision Surfaces

nominally located at $\mu_1(\mu_2)$, will be hyperspheres centered at $\mu_1(\mu_2)$.

Assume we are given a sensed map X = (x_1 , X_2), and we must decide whether it should be assigned to RM(i) represented by μ_1 or RM(j) represented by μ_2. Given the situation described above, a minimum error decision procedure would be to compute $d(x, \mu_1)$, $d(x, \mu_2)$ and

$$\begin{bmatrix} \text{Assign X to RM(i) if } d(x,\mu_1) \leq d(x,\mu_2) \\ \text{Assign X to RM(j) if } d(x,\mu_1) > d(x,\mu_2) \end{bmatrix} \quad [2]$$

In terms of the signal space representation, we can partition signal space by a hyperplane (dashed line in Fig. 4a) which is the perpendicular bisector on the line joining μ_1 and μ_2. Then if X falls on the same side of the hyperplane as $\mu_1(\mu_2)$, we assign it to $\mu_1(\mu_2)$.

Figure 4b depicts a situation in which we know or assume that our measurement of X2 is less reliable (or subject to more variation) than x_1 . Note that in this case the equiprobability contours are elliptical with the long axis in the X_2 direction. We can restore the situation of Fig. 4a if we scale each X_i by a quantity inversely related to our uncertainty in its true or nominal value. This scaling results in a modified distance measure:

$$d'_{ij} = \left\{ \sum_{k=1}^{N} \left[(y_{ik}/\sigma_k) - (y_{jk}/\sigma_k) \right]^2 \right\}^{1/2} \quad [3]$$

We then have an optimal decision procedure identical in form to that given in relation [2] with d replaced by d' .

Figure 4c illustrates the situation in which the disturbances affecting x_1 and X_2 are not independent. In this case, since an error in x_1(X2) implies something about the error affecting $x_2(X_1)$, the symmetry axes of our equiprobability contours will no longer be parallel to the coordinate axes. We note that if X_1 and x_2 are positively correlated, and $\sigma_1 = \sigma_2$, the major axis of the equiprobability contours will have a 45° angle to the x_1 coordinate axis.* To retain the decision rule given in [2] , we must further revise the distance measure to effectively eliminate the interactive effects. In particular, a general linear transformation is required to rotate the coordinate frame so that its axes are parallel to those of the ellipsoids. The coefficients TJK for this transformation can be approximated by the elements of a matrix which is the inverse of the covariance matrix of the X_i . In functional form, we then have:

$$d''_{ij} = \left[\sum_{\ell=1}^{N} \sum_{k=1}^{N} \tau_{\ell k}(x_{ik} - x_{jk})(x_{i\ell} - x_{j\ell}) \right]^{1/2} \quad [4]$$

*For the bivariate normal distribution, the angle of inclination of the major axis to the x_1 coordinate axis can be shown to be $\theta = 1/2 \arctan\left[\rho\sigma_1\sigma_2/(\sigma_1^2 - \sigma_2^2)\right]$.

Thus, we see that under rather general conditions, the optimal decision procedure (given by [2]) in deciding how to assign an unknown object to one of two possible categories is to measure the adjusted signal space distance (given by f 1), [3], or [4]) between the object (SM) and the expected values of the ideals representing the two categories [RM(i) and RM(j)J . To decide between R possible categories, we can make (R - 1) binary decisions, each time eliminating the least likely alternative.

The conceptual generality of the signal space approach has a number of practical limitations. To a large extent, these can be summarized by saying that the model is useful only in reasonably well controlled situations where the errors are small and random. Because these conditions can be met in many applications involving the detection of scene congruence, the signal space approach is very powerful.

Let us now consider the significance of the quantities that appear in the "distance" expressions. The first quantity we wish to consider is μ_1 , the expected value of RM(i) . The noise-free representation of RM(i) has been defined as Y_i = (y_{i1} , y_{i2} . . . . . yiN) However, as we shall observe shortly, most of the error processes to be considered have a biasing** effect on the expected signal space location of RM(i) . Further, it is desirable to normalize RM(i) when we expect to encounter significant signal variations (such as amplitude gain and bias variation) whose parameters we will not or cannot estimate. Normalization changes the expected signal space location of RM(i) in a known way.

The quantity σ_k, associated with the kth sample of any SM, is a measure of the total unbiased variation we can expect to encounter in attempting to measure yy^ . In a more general formulation, we could consider this variation to be a function of the RM(i) as well as the sample index (k) . However, in this treatment we assume that the functional dependence of *a* on RM(i) is unknown and thus heuristically assumed to be uniform over all RM(i) In the presence of scale and rotation error, σ_k will be a function of k in a manner derived in Appendix C.

The quantity $\rho_{\ell k}$ is a measure of the linear dependence of the noise acting on the ith sample to the noise acting on the kth sample. (It in no way reflects on the relationship between the expected values of the samples themselves.)

Given the orientation of the applications to which this paper is directed, it will not be practical in general to attempt to determine the values of the $\tau_{\ell k}$ appearing in [4) . Thus, we will typically ignore the interactive effects and pay the associated error penalty; or we will assume some simple structure for the $\rho_{\ell k}$ and attempt to compensate for the interaction. For example, a reasonable assumption might be that the noise

**We will define biased noise as any noise or distortion process that has the effect of shifting the expected location of RM(i) in signal space.

interaction between any two samples in the SM falls off exponentially with their separation. This assumption is discussed in Ref. (4).

Scale Change and Rotation Error

Analysis of the effects of scale and rotation errors is a major theme in this paper. If the SM and its corresponding RM(t) are translated into best alignment under scale and rotation error, it is obvious that cells near the map centers (i.e., the true match point) will be in better registration than the cells on the map periphery. This point is illustrated in Fig. 5a, and a method for computing overlap is presented in Appendix C. The two main consequences of this phenomenon are:

(1) There is an upper limit on the effective size of a SM. (This point is discussed in Appendixes B and C and the section on Extreme Distortion.)
(2) The reliability of measurements falls off as distance from the map center increases. Thus, distance metric [3] should be employed in applying optimal decision rule [2]. This result is formally derived for the Gaussian case in Appendix B.

Another result of the inability to completely align the SM with its RM(t) is the introduction of biased noise. That is, to the extent that two corresponding cells (one in the SM and one in the RM) do not overlap, a random component having the same statistics as the composite RM is added to the SM (see Eq. [B.1]) and thus the expected value of every individual RM(i) is biased toward the point in signal space corresponding to

$$\left(\frac{1}{R}\sum_{k=1}^{R} Y_k\right)$$

as illustrated in Fig. 5b. The result of this biasing is to reduce the signal space distance between any two RM(i) and thus increase the probability of error in distinguishing between them. In the discussions on map normalization in the following sections, it is important to note that it is the expected value (μ_i) of RM(i), and not Yi, that is being normalized.

Amplitude Gain Error

Figure 6a illustrates the effect of an amplitude gain change on expected match point error. For no gain variation (G = 1), let RM(1) and RM(2), with expected values μ_1 and μ_2, be alternative match point possibilities. Assuming that the sample variables have been properly scaled to equalize their variation, the hyperplane which is the perpendicular bisector of the line joining μ_1 and μ_2 is chosen as the decision surface corresponding to optimal decision rule (2) with distance metric (1). Under a gain change α, all vectors μ_i are extended radially out from the origin to new locations $(\alpha\mu_i)$ The optimal decision surface now becomes the hyperplane which is the perpendicular bisector of the line joining $(\alpha\mu_1)$ and $(\alpha\mu_2)$ In general, the new and old decision surfaces will not coincide, and any SM falling into the region between

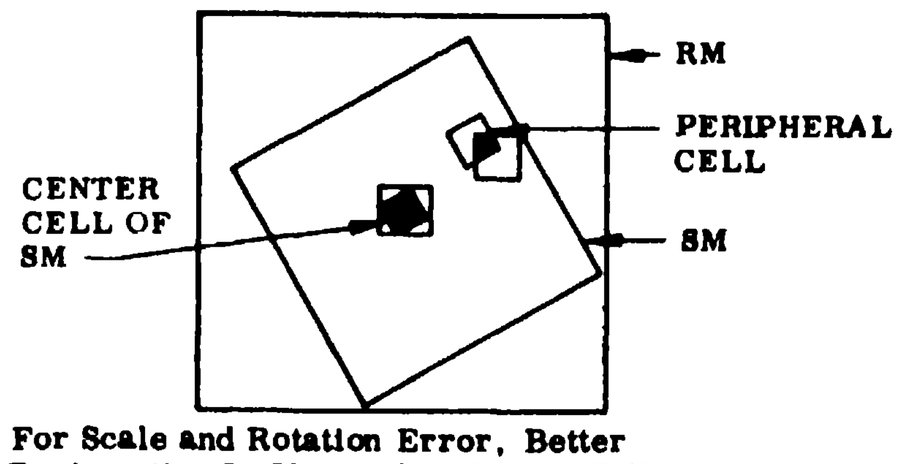

a. For Scale and Rotation Error, Better Registration Is Obtained at Center Cells of SM Than at Peripheral Cells

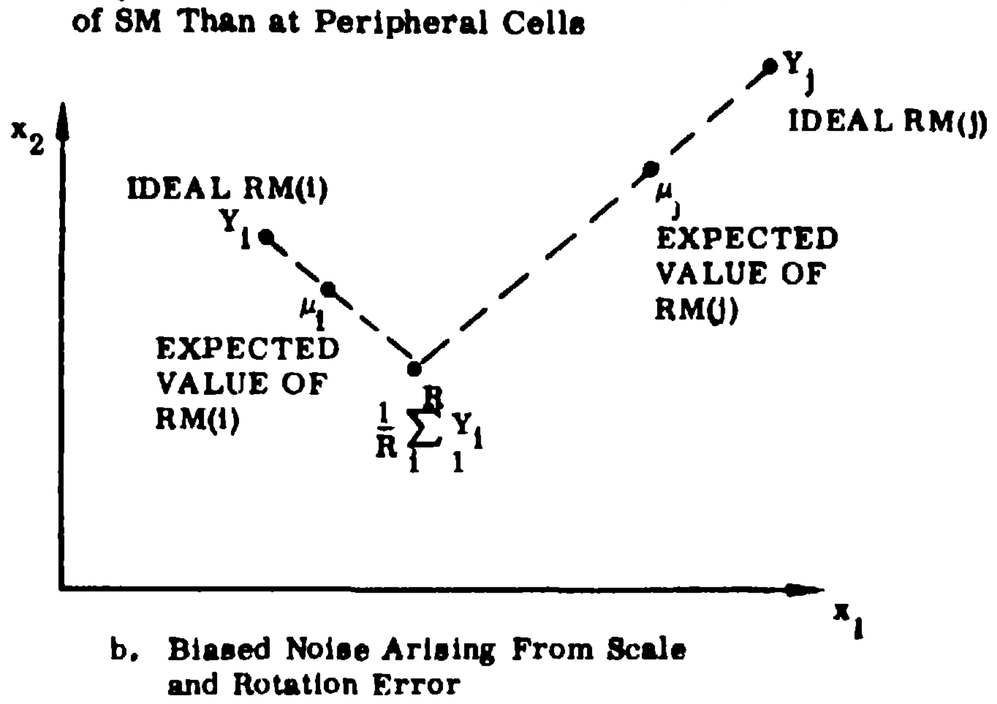

b. Biased Noise Arising From Scale and Rotation Error

Fig. 5 Effects of Scale and Rotation Error

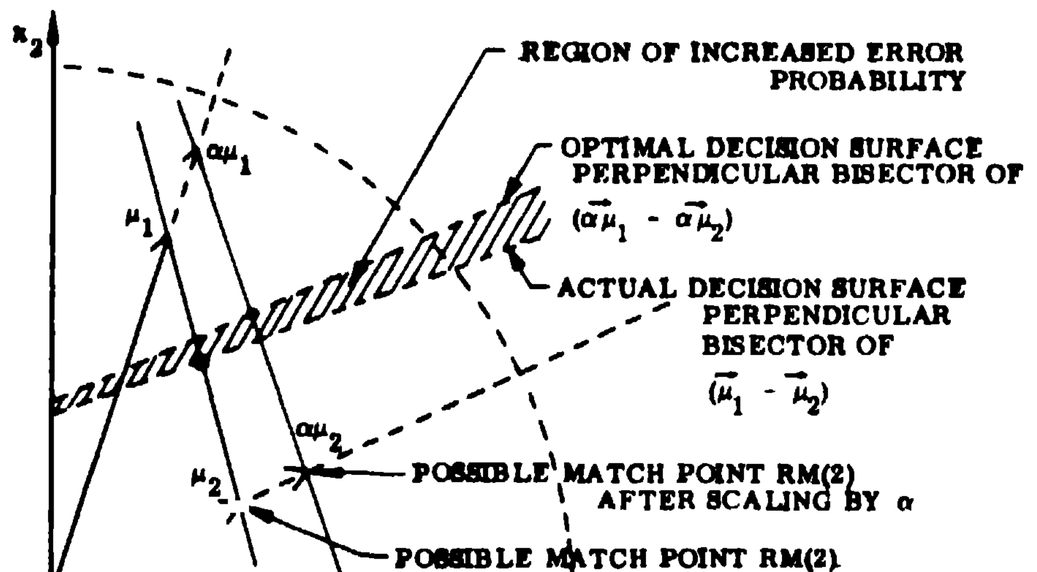

a. Effect of an Amplitude Gain Change on Expected Match Point

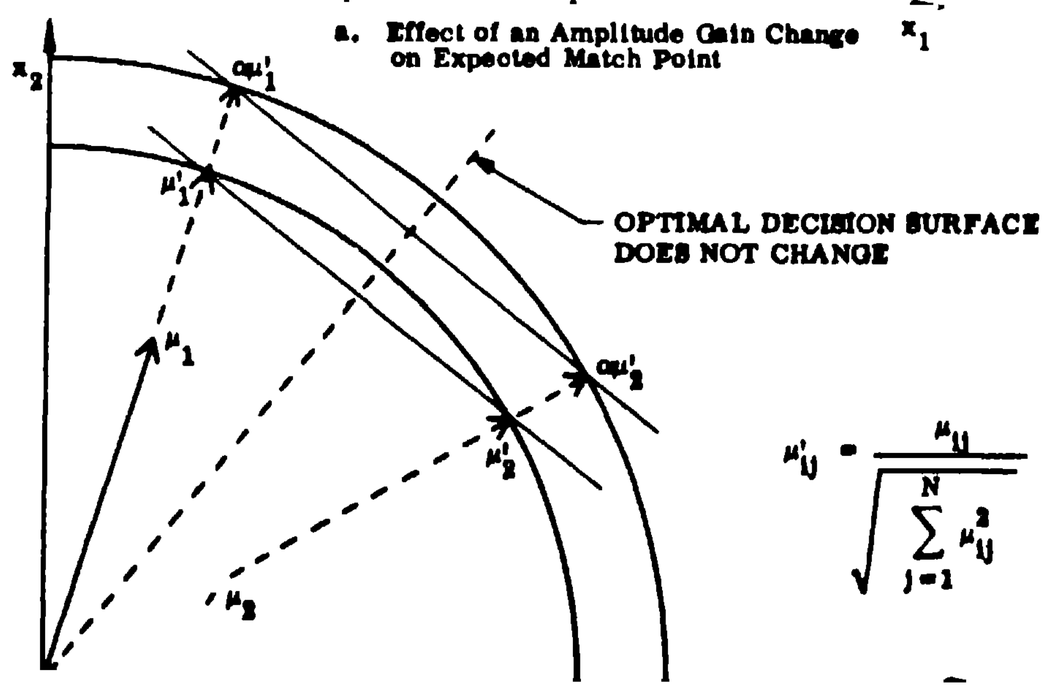

b. Effect of "Energy" Normalization on Amplitude Gain Error

Fig. 6 Normalization for Uniform Amplitude Gain Error

them (shaded in Fig. 6a) will be classified in a nonoptimal manner.

Figure 6b illustrates the effect of "energy" normalization on amplitude gain error. If RM(1) and RM(2) are normalized by dividing each of their sample values μ_{ik} by

$$\left(\sum_{k=1}^{N} \mu_{ik}^2 \right)^{1/2}$$

then they will have expected values μ_1' and μ_2', where μ_1' and μ_2' lie on the same hypersphere centered at the origin of the signal space coordinate system. The optimal decision surface in this case can be seen to bisect the angle θ formed by μ_1'-origin-μ_2' If a gain change α occurs, the angle between $\alpha\mu_1'$-origin-$\alpha\mu_2'$ *in* still θ and the new optimal decision surface coincides with the old. Thus, the optimal decision surface chosen for energy-normalized maps remains invariant under a gain change. It can also be shown that the expected error for energy-normalized maps is invariant under gain change. These assertions are verified for the case of Gaussian noise in Appendix B. However, in Appendix A it is shown that energy normalization itself raises the probability of error over the unnormalized case when no gain variation is possible.

Amplitude Bias Error

Figure 7 illustrates the effect of an amplitude bias error. For no bias variation, let RM(1) and RM(2), with expected values μ_1 and μ_2, be alternative match point possibilities. Assuming that the sample variables have been properly scaled to equalize their variation, the hyperplane which is the perpendicular bisector of the line joining μ_1 and μ_2 is chosen as the decision surface corresponding to rule (2) with distance metric (1). Under a uniform bias error $\vec{\beta} = b(1, 1, \ldots, 1)$, all vectors μ_i are displaced in a direction parallel to $\vec{\beta}$ ($\vec{\beta}$ makes a 45° angle with each of the coordinate axes) to new locations $(\vec{\mu}_i + \vec{\beta})$ The optimal decision surface now becomes the hyperplane which is the perpendicular bisector of the line joining $(\vec{\mu}_1 + \vec{\beta})$ and $(\vec{\mu}_2 + \vec{\beta})$ In general, the new and old decision surfaces will not coincide, and any SM falling in the region between them (shaded in Fig. 7) will be classified in a nonoptimal manner.

If bias normalization is employed, a vector $\vec{\alpha}_{\mu i} = k_{\mu i}(1, 1, \ldots, 1)$, which makes a 45° angle with each of the coordinate axes, is added to each $\vec{\mu}_i$ so that $(\vec{\alpha}_{\mu i} + \vec{\mu}_i) = \vec{\mu}_i'$, where $\mu_i' = (c_{i1}, c_{i2}, \ldots, c_{in})$ and

$$\sum_{k=1}^{N} c_{ik} = 0$$

It can now be seen that all $\vec{\mu}_i'$ lie in the hyperplane normal to the unit vector $\vec{\beta}' = (1, 1, \ldots, 1)$. That is:

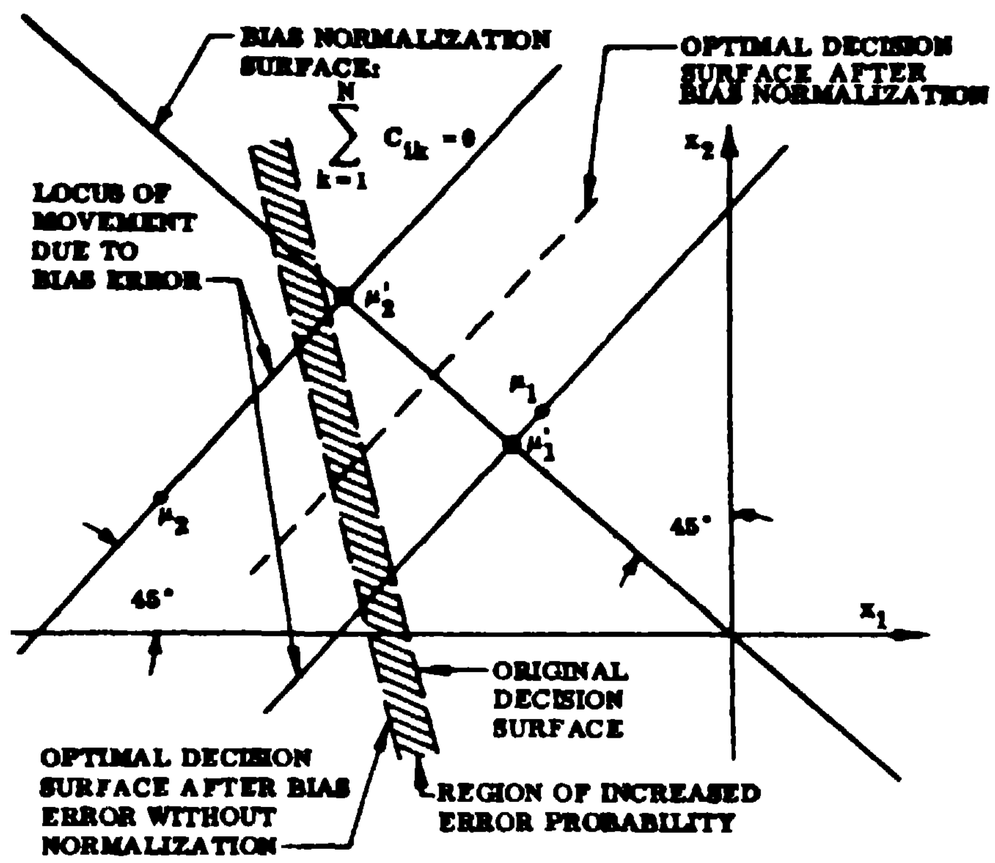

Fig. 7 Normalization for Uniform Bias Error

$$(\vec{\beta}', \vec{\mu}_i') = \sum_{k=1}^{N} c_{ik} = 0$$

Thus, the hyperplane γ which is the perpendicular bisector of the line joining $\vec{\mu}_1'$ and $\vec{\mu}_2'$ is parallel to any bias vector $\vec{\beta}$ The effect of $\vec{\beta}$ acting on $\vec{\mu}_1'$ and $\vec{\mu}_2'$, then is simply to move $\vec{\mu}_1'$ and $\vec{\mu}_2'$ along paths parallel to γ and thus leave γ unaltered. Thus, the optimal decision surface chosen for maps with zero mean value remains invariant under a uniform bias change.

It is worth noting at this point that under nonuniform bias change, the appropriate normalization is to spatially differentiate (perhaps more than once) the maps. In the limiting case, this could result in a two-level binary map in which intensity contours would provide the necessary information. For such a scheme to be effective, noise cleaning techniques which eliminate high-frequency noise without blurring edges would have to be applied to the differentiated maps prior to match point determination.

Remote Error

It is useful to consider two distinct types of error processes. The first type, which we shall call "Accuracy Errors" (AE), are local deviations about the "true" match point, and reflect the fact that physically adjacent maps will have small signal space separation due to system bandwidth limitations. We define a second class of errors, called "Remote Errors" (RE), which correspond to falsely detecting a match at a point typically remote from the true match point. An RE can arise due to the chance occurrence of more than one area in the RM closely resembling the SM.

Thus, we define Remote Error (RE) as the chance occurrence of a RM(g) sufficiently close (in signal space) to the "true" RM(t) so that RM(g) falls into the expected sphere of error surrounding RM(t).

We can now determine that probability of a remote error as follows: Let us assume that the maximum number of distinct RM(i) is DM (see Appendix A) * Then the probability of a remote error for a RM with R components is:

$$Pr[RE] = 1 - \left[1 - \sum_{t=1}^{(DM)} Pr(t)\, Pr(g|t)\right]^{R}$$

By the statement of the problem, Pr(g| t) = Pr(g)

For the case where all distinct RM(i) are equally likely to occur, we have:

$$Pr[RE] = 1 - [1 - (1/DM)]^{R}$$

For [(DM) -> 1] :

$$Pr[RE] \approx (R/DM) = R[1 + (\hat{P}/\sigma^2)]^{-N/2}$$

where $\hat{P}$ is the maximum value of the average signal power in a RM(i), σ^2 is the average noise power, N is the number of independent samples in a SM, and R is the number of elements in the RM less the number of elements in the SM .

Thus, we see that the approximated probability of a RE is proportional to the size of the RM, but in a stronger sense is inversely related to the size of the SM and the signal-to-noise ratio. In particular, a large number of independent samples can assure a very low probability of remote error.

In some applications, it may be possible to reduce the probability of RE by rejecting any match point decision which does not exceed a confidence level based on the relative "cost" of a RE versus the "cost" of no decision (or reject). Reference (5) presents an analysis of this situation.

Scene Characterization and Scene Selection

Scene characterization is defined as a number associated with a scene which rates the probable effectiveness of the scene in terms of its ability to minimize match point error. The importance of such a characterization derives from the fact that in many applications in which the scene congruence problem arises, scene selection is a parameter which can be optimized. For example, in map matching for navigation and guidance, the ground reference scene (RM) may be freely chosen, and we might even have some latitude in choosing the SM .

Based on the definition given above, one appropriate scene characterization measure would be the expected probability of digital match point error using the given scene. In this sense, Eq. [B.II] or[B.13] can be used for scene characterization. We note that any useful measure tor scene characterization is meaningful only with respect to a particular decision procedure and noise environment. If the noise environment is assumed constant, then the "average weighted signal space distance (D')" between a RM(i) and one of its immediate neighbors (see Eq. [B. 14]) can be computed directly from a given scene and used as the desired metric.

In a situation in which we can choose among a large selection of possible scenes, the computational complexity of a scene characterization measure can be a critical factor. For rough or initial screening. Eq. [B.14] can be approximated by simply measuring the sum of the squared difference of adjacent samples in the x and y directions. (These measures will be called the x and y Variation while the measures corresponding to Eq. IB. 14] will be called the Weighted Variation.) The following table gives the results of some preliminary experiments** on the correspondence between Weighted Variation and match point error for a fixed error package and decision rule Eq. [B.6] .

Scene Number	x Displacement Error	y Displacement Error	$\left(\text{x Weighted Variation}\right)^2$	$\left(\text{y Weighted Variation}\right)^2$	SM Size	RM Size
1	0	1	30	1	16^2	32^2
2	1	1	1	5	16^2	32^2
3	0	0	58	386	16^2	32^2
4	1	1	12	42	18^2	40^2
5	0	0	235	169	18^2	40^2
6	1	0	18	11	18^2	40^2
7	1	0	13	7	18^2	40^2
8	0	0	112	476	36^2	48^2
9	0	0	296	129	36^2	56^2

It can be seen that for the particular error package employed, a map with a (squared) Weighted Variation of 50 or more in the x or y direction had no displacement error in the corresponding direction.

To a large extent, Variation measures are also measures of the high frequency content of a map. It is intuitively reasonable to expect that a potential for very accurate positioning should be dependent on the presence of a significant amount of high (spatial) frequency energy in the scene. Further, for a given sampling rate, the relative independence of the measurements increases as a function of the high frequency content of the map. Thus, a high Variation measure also implies a lower probability for remote error.

As noted earlier, errors due to gain or bias changes can be minimized by either normalizing the scenes (both SM and RM) with respect to average value and to "energy" content, or by choosing scenes which are relatively uniform in these quantities. Thus, in addition to the proposed Variation measures, additional measures relating how statistically uniform the scene is can provide useful information.

*It is important to distinguish between the RM(i) which are the components of some given Reference Map (and not necessarily distinct), and a catalog of all possible RM(i) which are distinct.

**Data used in these experiments were obtained from aerial photography of the San Francisco Bay Area.

EXTREME DISTORTION

It has been noted that one effect of scale change and rotation error is to produce a "decorrelating" phenomenon as scene or map size increases. Thus, under scale and rotation error, there is an upper limit to the useful size of a coherent map (see Appendix C). Unfortunately, SM size is the parameter that offers the greatest latitude for maintaining or improving match accuracy in the presence of excessive noise.

The Concept of SM Decomposition

One solution to the problem of extreme distortion is to acquire a large sensed map, and decompose it into segments of not greater than critical size. Each of these segments is applied separately to locate a match point, and the set of match points then combined (by a curve-fitting technique, such as direct or weighted averaging, least squares, etc.) either to derive a best estimate match point or to estimate the actual scale and rotation error. In the latter case, the sensed map can be computationally adjusted to eliminate the existing scale and rotation factors, thus allowing the entire sensed map to be applied coherently. (The process of error estimation and correction can be applied iteratively as many times as desired.)

Figure 9 illustrates some of the above concepts. In Fig. 9a we depict a situation in which the SM is a rotated contracted version of its intended image in the RM In Fig 9b we see that if the SM is treated as a coherent entity, and if region A of the SM is in proper registration, then region B of the SM will be correlated with the top left corner of the RM , resulting in a low correlation score. However, it the SM is decomposed into subregions (nine are shown in this example) and each subregion independently correlated, a pattern of match points similar to that shown in Fig 9c will be obtained. From this pattern we can estimate the desired parameters (i.e., match point, rotation error, scale factors).

The Linear Case*

Given a correlation pattern similar to that of Fig. 9c, a curve-fitting technique such as least squares forces us to assume something about the distortion process which produced the given pattern. The simple assumption made up to this point is that the distortion process is linear and thus we would look for the best rectangular (or square) grid which fits the pattern in Fig. 9c in a least squares sense. The center of the grid is the desired match point, while the slope and stretching of the grid specify the corresponding rotation and scale errors in the associated SM .

If a remote error occurred in one or more of the match points in the correlation pattern given in Fig. 9c, a rather large error could be introduced into our

The concept of SM decomposition and its use in linear parameter estimation were independently arrived at by Lynn Quam of Stanford University. He is currently preparing a Ph.D. dissertation which will include his results in this area.

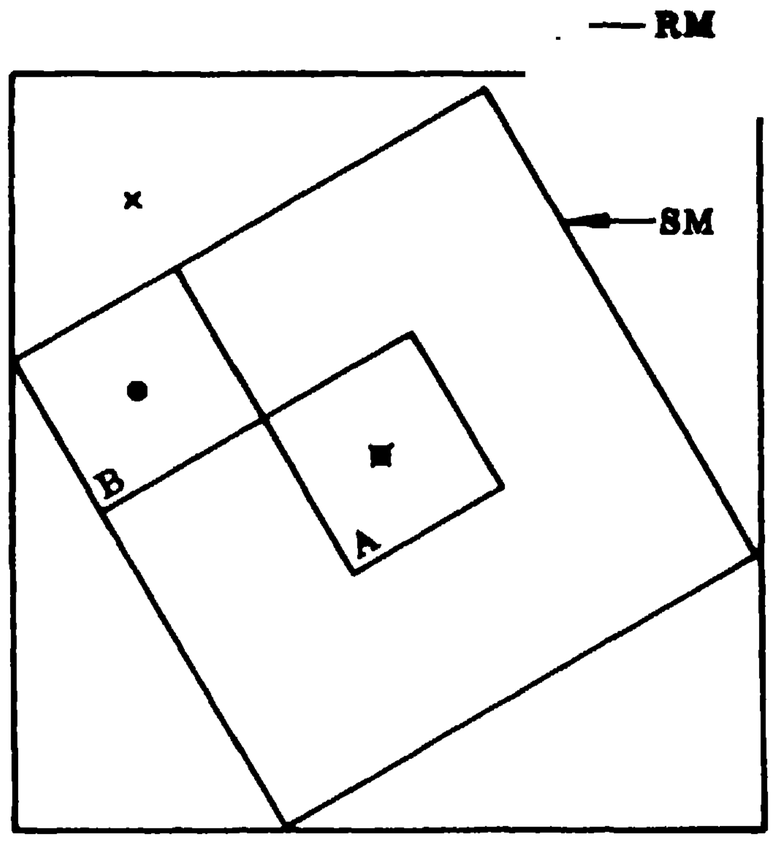

a Situation Using Large SM When Rotation and Contraction Errors Are Present

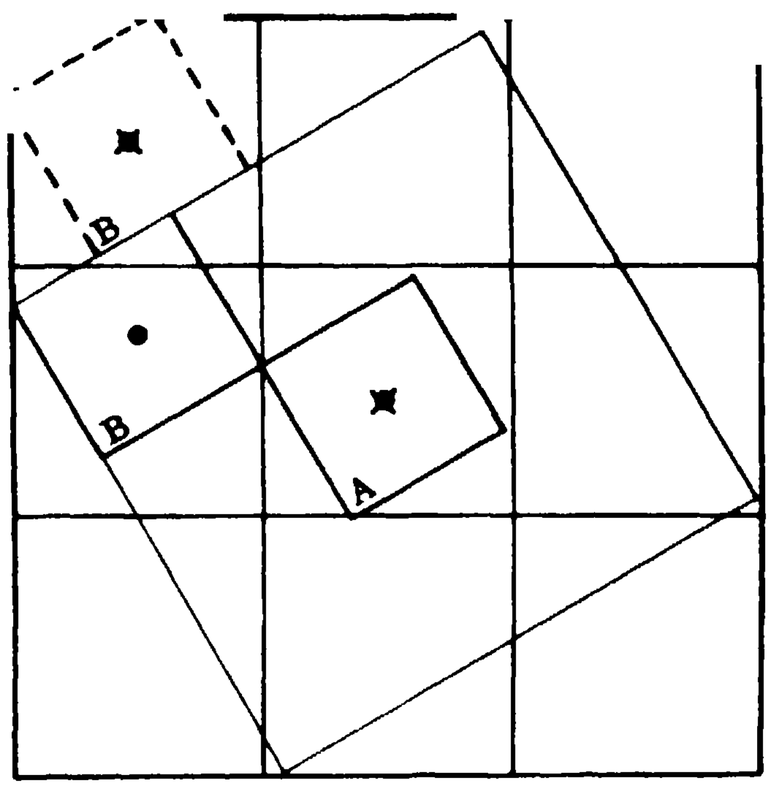

b Dashed Square Indicates Subregion of SM Correlated Without Decomposition (i.e., Coherent Correlation)

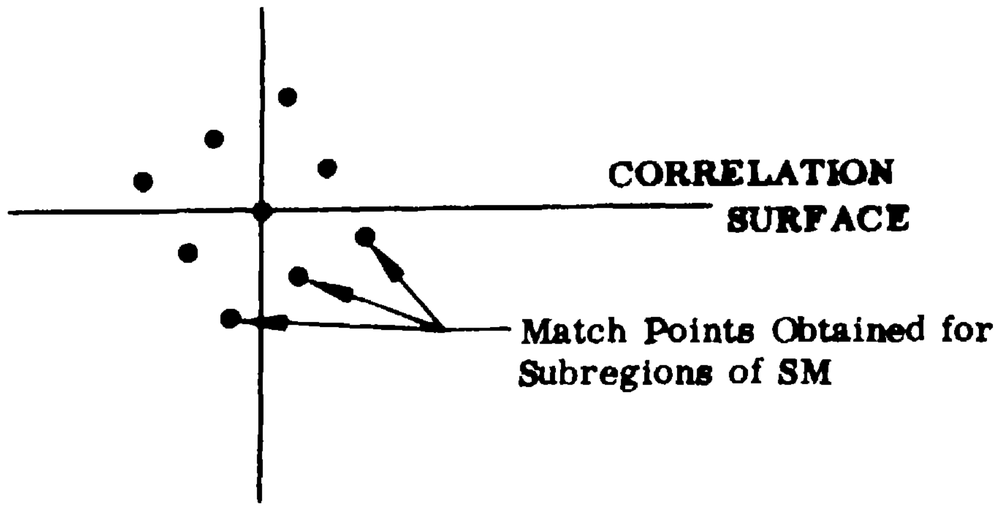

c. Set of Match Points Obtained for Independently Correlated SM Subregions

Fig. 9 Decomposition of the Sensed Map To Reduce Scale and Rotation Error

parameter estimates. Therefore, it is desirable to employ some type of "clustering" technique which will permit us to eliminate "wild" points prior to making the least squares estimate.

The "Rubber Sheet" Case

In many problems of interest, the linear distortion assumption of the preceding section would not be adequate. More to the point, we are frequently faced with a situation in which it is not possible to offer a completely defined distortion mechanism suitable for probabilistic analysis. In this case, we must first offer a procedure for locating the SM image in the RM ; and then provide a second procedure for finding the match point as a function of this RM image.

Without a model for probabilistically relating a SM (or segment thereof) to a RM, we must (heuristically) select a distance measure to be used as the basis for classification. Consider some metric $\psi_k(y_j)$ which defines the "distance" between the kth element of the SM and the jth element of the RM* Let us now consider the use of this metric with the rather general class of distortion processes which sequentially constrain the elements of the SM . That is, for any given SM element xk, a constraint (ft) is placed on the region in which x_{k+1} can lie. We now define the RM image of the SM to be that collection of yj for which

$$\left[\sum_{k=1}^{N} \psi_k(y_j)\right] \qquad [15]$$

is minimized subject to a sequential constraint on the x_k.

Evaluation of metric Eq. [5] can be accomplished conceptually (but not practically) by selecting N elements at a time from the RM and determining if they satisfy the constraint (Ω) For those N-tuples which do satisfy (Ω), we select the one which minimizes metric Eq. [5] as the required RM image of the SM .

A procedure (which is comparable in computation time to conventional correlation), has been devised for finding the RM image of the SM, and is presented below.

Let the RM be represented by the sequence

$$Y = \{y_1, y_2, \ldots, y_M\}$$

and let the SM be represented by the sequence

$$X = \{x_1, x_2, \ldots, x_N\}$$

Assume we are given a distance function ψ ; a sequential constraint set Ω; and we are asked to find the best (according to ψ and Ω) embedding of X in Y .

*In general, ψ_k can also be a function of the physical distance between the embedded locations of xk and X_{k-1}, X_{k-2} ....,X_1

Consider an M x N tableau where the rows are indexed by the elements of Y and the columns by successively larger subsequences of the elements of X .

We now define the following quantities:

$\alpha_1^{j,k}$ = the best way of embedding the first (k - 1) elements of X into the first (J - 1) elements of Y, given that x_k is assigned to y_j

$\alpha_2^{j,k}$ = a k-tuple giving the k locations in Y corresponding to the embedding given by $\alpha_1^{j,k}$

$\alpha_3^{j,k}$ = the best embedding of the first k elements of X in the first j elements of Y, without necessarily assigning x_k to y_j

$\alpha_4^{j,k}$ = a k-tuple giving the k locations in Y corresponding to the embedding given by $\alpha_3^{j,k}$

$\omega_{j,k}$ = the set of possible embeddings of x_{k-1} given that x_k is embedded in location j

$$\alpha_1^{j,k} = \psi_k(y_j) + \min_{i \epsilon \omega_{j,k}} \left\{\alpha_1^{i,k-1}\right\}$$

$$\alpha_1^{j,1} = \psi_1(y_j)$$

$$\alpha_2^{j,k} = \left[\alpha_2^{j^*,k-1}, j\right] \text{ where } j^* \text{ is chosen so that}$$

$$\alpha_1^{j^*,k-1} = \min_{i \epsilon \omega_{j,k}} \left\{\alpha_1^{i,k-1}\right\}$$

$$\alpha_3^{j,k} = \min\left[\alpha_3^{j-1,k}, \alpha_1^{j,k}\right]$$

$$\alpha_3^{1,k} = \alpha_1^{1,k}$$

$$\alpha_4^{j,k} = \{j_i\} : \sum_{i=1}^{k} \psi_i\left(y_{j_i}\right) = \alpha_3^{j,k}$$

The (j k) entry in the tableau is

$$\left[\alpha_1^{j,k}, \alpha_2^{j,k}\right]$$

We append a final column to the tableau whose jth row entry has the form

$$\left[\alpha_3^{j,N}, \alpha_4^{j,N}\right]$$

The "best" embedding is then given by $\alpha_4^{M,N}$, and the "distance" between X and its image in Y is given by $\alpha_3^{M,N}$

The example presented in Fig. 10 illustrates the operation of the above algorithm. The constraint set selected for this example would include the case where the scene was stretched by pulling outward on the upper left and lower right corners of a rubber sheet containing the scene.

$Y =$ | 3 | 5 | 3 |
| 5 | 1 | 6 |
| 7 | 5 | 8 |

$\phi_k(y_j) = |x_k - y_j|$

$\omega_{(a,b),k} = \{(a, b-1), (a-1, b)\}$

$X = (2, 5, 8)$

j	$\omega_{j,k}$	(x_1) $\alpha_1^{j,1}$	$\alpha_2^{j,1}$	(x_1, x_2) $\alpha_1^{j,2}$	$\alpha_2^{j,2}$	(x_1, x_2, x_3) $\alpha_1^{j,3}$	$\alpha_2^{j,3}$	$\alpha_3^{j,3}$	$\alpha_4^{j,3}$
1 = (1, 1)	–	1	1	–	–	–	–	–	–
2 = (1, 2)	1	3	2	0 + 1 = 1	1, 2	–	–	–	–
3 = (1, 3)	2	1	3	2 + 3 = 5	2, 3	5 + 1 = 6	1, 2, 3	6	1, 2, 3
4 = (2, 1)	1	3	4	0 + 1 = 1	1, 4	–	–	6	1, 2, 3
5 = (2, 2)	2, 4	1	5	4 + 3 = 7	2, 5	7 + 1 = 8	1, 2, 5	6	1, 2, 3
6 = (2, 3)	3, 5	4	6	1 + 1 = 2	3, 6	2 + 5 = 7	2, 3, 6	6	1, 2, 3
7 = (3, 1)	4	5	7	2 + 3 = 5	4, 7	1 + 1 = 2	1, 4, 7	2	1, 4, 7
8 = (3, 2)	5, 7	3	8	0 + 1 = 1	5, 8	3 + 5 = 8	4, 7, 8	2	1, 4, 7
9 = (3, 3)	6, 8	6	9	3 + 3 = 6	8, 9	0 + 1 = 1	5, 8, 9	1	5, 8, 9

Fig. 10 An Example of Two-Dimensional Embedding

For some applications, we might expect parts of the scene to remain coherent while other parts undergo "rubber sheet" distortion. This situation can be handled by the preceding algorithm by simply allowing certain of the x_i to represent fixed arrangements of resolution elements, rather than single elements. This point is illustrated in the example of Fig. 11.

$Y =$ | 3 | 5 | 3 |
| 5 | 1 | 6 |
| 7 | 5 | 8 |

$X = (\boxed{2}\ \boxed{5}, 8)$ i.e., x_1 is the coherent horizontal configuration $\boxed{2}\ \boxed{5}$ and $x_2 = 8$.

$\omega_{(a,b),k} = \{(a, b-1), (a-1, b)\}$ where we use the cell marked by an arrow in x_1 to interpret the constraint relations.

$\phi_k(y_j) = |x_k - y_j|$

j	$\omega_{j,k}$	(x_1) $\alpha_1^{j,1}$	$\alpha_2^{j,1}$	(x_1, x_2) $\alpha_1^{j,2}$	$\alpha_2^{j,2}$	$\alpha_3^{j,2}$	$\alpha_4^{j,2}$
1 = (1, 1)	–	–	–	–	–	–	–
2 = (1, 2)	–	1	2	–	–	–	–
3 = (1, 3)	2	5	3	5 + 1 = 6	2, 3	6	2, 3
4 = (2, 1)	–	–	–	–	–	6	2, 3
5 = (2, 2)	2	7	5	7 + 1 = 8	2, 5	6	2, 3
6 = (2, 3)	3, 5	2	6	2 + 5 = 7	3, 6	6	2, 3
7 = (3, 1)	–	–	–	–	–	6	2, 3
8 = (3, 2)	5	5	8	3 + 7 = 10	5, 8	6	2, 3
9 = (3, 3)	6, 8	6	9	0 + 2 = 2	6, 9	2	6, 9

Fig. 11 An Example of Two-Dimensional Embedding With Coherent Objects and Rubber Sheet Distortion

For a RM with M elements and a SM with N elements, simple correlation would require on the order of kMN computations where k is a constant of proportionality which takes into account one multiplication and one or more additions and subtractions. For the algorithm given above, the number of computations is still proportional to MN, where the constant of proportionality is now determined by both the distance metric (ψ) and the constraint set (Ω)

Given that we have successfully embedded the distorted RM in the SM, the need to locate a specific match point (i.e., the point in the RM at which the sensor is pointing) might not be relevant and, in fact, might not even be meaningful. However, if this requirement does exist, then the match point can be determined by comparing the resulting configuration to a number of stored models for distortion, all of which are subsumed by Ω A best fit to one of these models would then determine the specific procedure which derives the match point from the embedded SM.

The algorithm for rubber sheet distortion has a one-dimensional version which offers significant simplifications. Let us consider the constraint set

$$\omega_{jk} = \{j' \mid j' < j\}$$

i.e., we have a situation in which the sequence representing the RM is stretched relative to the SM. In a practical situation, if it is not clear whether the SM has shrunk or expanded, the desired situation can be obtained by linearly "stretching" the RM sequence.

In the tableau for the one-dimensional version of the algorithm, we can replace $\alpha_1^{j,k}$ and $\alpha_2^{j,k}$ with $\alpha_3^{j,k}$ and $\alpha_4^{j,k}$ as column heads for all k; further we now have, $\alpha_1^{j,k} = \psi_k(y_j) + \alpha_3^{j-1,k}$. Figure 12 illustrates the one-dimensional case.

$Y = (2, 1, 2, 1, 2)$ $\quad \psi_k(y_j) = |x_k - y_j|$

$X = (1, 2, 3)$ $\quad \alpha_3^{j,k} = \min\left[\alpha_3^{j-1,k}, |x_k - y_j| + \alpha_3^{j-1,k-1}\right]$

$\omega_{j,k} = \{j' \mid j' < j\}$ $\quad \alpha_4^{j,k} = \{j_l\} : \sum_{l=1}^{k} \psi_l(y_{j_l}) = \alpha_3^{j,k}$

j	(x_1) $\alpha_3^{j,1}$	$\alpha_4^{j,1}$	(x_1, x_2) $\alpha_3^{j,2}$	$\alpha_4^{j,2}$	(x_1, x_2, x_3) $\alpha_3^{j,3}$	$\alpha_4^{j,3}$
1	1	1	–	–	–	–
2	0	2	2	1, 2	–	–
3	0	2	0	2, 3	3	1, 2, 3
4	0	2	0	2, 3	2	2, 3, 4
5	0	2	0	2, 3	1	2, 3, 5

Fig. 12 An Example of One-Dimensional Embedding

SUMMARY

It is shown that the scene congruence problem can be formulated as a classification problem in a suitably defined signal space; this allows both geometric analysis, and the application of decision theoretic methodology. It is then shown that an optimal procedure for match point determination will typically be based upon a weighted Euclidean distance metric. (See section on decision procedures and Eq. [B. 6] .)

The principal effect of scale and rotation error is shown to be a "decorrelating" effect as map size increases. This in turn results in an upper bound on the effective size of a sensed map which is a function of scale factor and rotation. (Match accuracy can

decrease if map size exceeds this critical size.) Further, the reliability of a sensed measurement decreases as its distance from the sensed map center increases. It is this nonuniformity which must be accounted for in the signal space distance metric. (See section on scale and rotation, Eq. [B.20] and Appendix C.)

Normalization techniques to minimize the effects of amplitude gain and bias error are presented, and their significance is geometrically analyzed. In particular, normalization involves the effective reduction of signal space dimensionality (and the consequent increase in remote error probability) to produce a situation where the corresponding error process no longer affects either the decision procedure or the error probability. (See sections on gain and bias error, remote error, and Appendix A.)

An analysis of the remote error problem shows that for signal-to-noise ratios greater than 1, the number of independent scene measurements is the predominant factor in assuring protection against remote error. (See section on remote error and Appendix A.)

It is shown that a scene property, closely related to the high spatial energy content of the scene, is a good indicator of the quality of the scene with respect to potential match point error, (See section on scene characterization and Eq. (B.14) .)

For the "large error" case, two alternatives are offered: sensed map decomposition in the case of linear distortion; and a new highly efficient algorithm which can be applied to "rubber sheet" distortion. (See section on extreme distortion.)

Appendix A (Abbreviated)

SIGNAL SPACE RELATIONS

If v(t) has duration T and bandwidth W then

$$E_v = \int_{-\infty}^{\infty} v^2(t)\,dt =$$

$$\int_{-\infty}^{\infty} \left[\sum_{n=-\infty}^{\infty} v(n/2W) \left[\sin(2\pi Wt - n\pi)/2\pi Wt - n\pi\right] \right]^2 \qquad [A.1]$$

$$E_v = 1/2W \sum_{n=0}^{2TW} [v(n/2W)]^2 \qquad [A.2]$$

$$d = \left(\sum_{n=1}^{N} v_n^2 \right)^{1/2} \qquad [A.3]$$

$$d^2 = 2WE_v = 2TW\bar{P}_v = N\bar{P}_v \qquad [A.4]$$

$$Vol \sim (d)^N \qquad [A.5]$$

$$DM = [1 + (\hat{P}/\sigma^2)]^{N/2} \qquad [A.6]$$

$$\tilde{DM} = [1 + (\bar{P}/\sigma^2)]^{N/2} \qquad [A.7]$$

$$\frac{\tilde{DM}}{DM} = (\bar{P}/\hat{P})^{N/2} \qquad [A.8]$$

where:

$N = 2TW$
$v_n = v(n/2W)$
$T\bar{P}_v = E_v$
d = Eucledian distance from signal to origin
E_v ~ Signal Energy
$\hat{P}$ ~ Peak Signal Power
$\bar{P}$ ~ Average Signal Power
σ^2 = Average Noise Power
DM = Number of Distinct Signals
$\tilde{DM}$ = Number of Distinct Signals After "Energy" Normalization
Vol = Volume of Hypersphere of Radius d

Appendix B (Abbreviated)

A BASIC ALGEBRAIC MODEL FOR DIGITAL MATCH POINT DETERMINATION

The purpose of this appendix is to verify and elaborate on geometrically derived conclusions, as well as to obtain specific numerical expressions under reasonable noise and distortion assumptions.

Optimum Decision Rule

Using the terminology and notion employed in the body of this paper,

$X = (x_1, x_2, \ldots x_N)$ is the sensed map (SM)

$Y_i = (y_{i1}, y_{i2}, \ldots y_{iN})$ is the ith reference map [RM(i)]

Let us assume the X is derived from RM(t). We make the following assumptions:

(1) Each component y_{ij} of the RM is an independent Gaussian random variable $[\mu_m, \sigma_m^2]$
(2) Each component x_i of the SM is derived from RM(t) in accordance with Eq. [B.1]:

$$X_j = \left(\phi_j y_{t_j}\right) + (1 - \phi_j)(W) + Z \qquad [B\ 1]$$

where Z is an independent Gaussian variable (arising from some external noise process) with mean μ_n and variance σ_n^2; W is an independent Gaussian random variable (associated with map element variation) with parameters μ_m, σ_m^2; ϕ is a function of the rotation angle θ, the scale change in the x direction α, the scale change in the y direction β, and the index j of the map element. In particular, ϕ_j is the percentage overlap of the jth SM element with its

corresponding RM element when the SM and corresponding RM are in best registration under the constraints imposed by scale change and rotation factors. Appendix C gives a procedure for evaluating ϕ

Assuming that the SM is equally likely to have been derived from any location in the RM, the decision procedure for minimum error is to assign X to RM(t) if:

$$\sum_{k=1}^{N} x_k \phi_k (y_{tk} - y_{ik})/\sigma_k^2 > 1/2 \sum_{k=1}^{N} \left(\mu_{tk}^2 - \mu_{ik}^2\right)/\sigma_k^2 \quad [B.6]$$

where

$$\sigma_k^2 = \sigma_n + (1 - \phi_k)^2 \sigma_m^2$$

$$\mu_{tk} = \phi_k y_{tk} + (1 - \phi_k)\mu_n + \mu_m$$

Then from Eq. [B.6] we can compute the probability of error Er[i|t] as:

$$Er[i|t] = \Phi\left\{-1/2\left[\sum_{k=1}^{N} \phi_k^2 (y_{tk} - y_{ik})^2/\sigma_k^2\right]^{1/2}\right\} \quad [B.10]$$

where Φ is the Gaussian cumulative distribution function:

$$\Phi(s) = \frac{1}{(2\pi)^{1/2}} \int_{-\infty}^{s} e^{-(1/2)y^2}\, dy$$

We then make the approximation:

$$\text{Total expected error} = \bar{E}r = 1 - \left[1 - \Phi\left(-\frac{1}{2}D'\right)\right]^M \quad [B.12]$$

and if $\Phi(-D'/2)$ is small, we have

$$Er \approx M\Phi(-D'/2) \quad [B.13]$$

where M is an empirical constant and

$$D' = \left[\sum_{k=1}^{N} \phi_k^2 (y_{tk} - y_{ik})^2/\sigma_k^2\right]^{1/2} \quad [B.14]$$

Decision rule Eq. [B.6] takes into account the biased noise effect produced by scale change and rotation errors. For practical reasons, it is sometimes desirable to ignore these effects and assume that $\phi_k = 1$ for all k. This simplification results in error probability (compare with Eq. [B.10]):

$$Pr[i|t] = \Phi\left(-\frac{\sum_{k=1}^{N} \frac{1}{2}(y_{tk} - y_{ik})[(1 - \phi_k)(2\mu_m - y_{tk}) + (\phi_k y_{tk} - y_{ik})]}{\left\{\sum_{k=1}^{N} \left[\sigma_n^2 + (1 - \phi_k)^2 \sigma_m^2\right](y_{tk} - y_{ik})^2\right\}^{1/2}}\right) \quad [B.20]$$

Note that all for k* such that $\phi_{k*} = 0$ (i.e., the k* elements in the SM and RM no longer have any area of overlap), the expected value of the summation in the numerator of Eq. [B.20] over the k* terms is zero. However, the contribution of these terms to the denominator is positive. This means that if the SM is made large enough so that ϕ_k becomes zero for part of the map, the resultant expected error is larger than that which would have resulted from using a smaller SM.

Consider a situation in which scale and rotation errors are absent, but assume that an uncompensated amplitude gain change can occur. The error probability in this case is (G = 1 for no gain error):

$$Pr[i|t] = \Phi\left\{-\frac{\left[\sum_{k=1}^{N} (y_{tk} - y_{ik})^2\right]^{1/2}}{2\sigma G} - \frac{(G-1)\left[\sum_{k=1}^{N} \left(y_{tk}^2 - y_{tk}y_{ik}\right)\right]}{\sigma G\left[\sum_{k=1}^{N} (y_{tk} - y_{ik})^2\right]^{1/2}}\right\} \quad [B.28]$$

For the case where RM(t) and RM(i) have equal energy

$$\left(\text{i.e., } \sum_{k=1}^{N} y_{tk}^2 = \sum_{k=1}^{N} y_{ik}^2\right)$$

a gain error can be ignored since it will not cause a change in the value of Eq. [B.28].

Appendix C (Abbreviated)

THE GEOMETRY OF SCALE AND ROTATION ERROR

The Overlap (Φ_k) Between Corresponding Elementary Areas in SM and RM Under Scale and Rotation

Suppose the Cartesian plane is subjected to scale and rotation changes. That is. it is expanded by a multiplying factor of α in the x-direction and β in the y direction (the origin being the fixed point in both oi these expansions), and then rotated counterclockwise about the origin by an angle of θ. Suppose further that R is a square centered at the point (x,y). which has sides parallel to the axes of the unexpanded, unrotated Cartesian plane and of length one, and that R' is R subjected to the above scale and rotation changes. We derive an expression approximating the area of $R \cap R'$

Subjecting the point (x, y), the center of R, to the given expansions yields the new point $(\alpha x, \beta y)$, and rotating $(\alpha x, \beta y)$ counterclockwise about the origin by θ yields the point (u, v), the center of R', where $u = \alpha x \cos\theta - \beta y \sin\theta$, and $v = \beta y \cos\theta + \alpha x \sin\theta$.

Let R" be the square whose sides are of length one and are parallel to the axes oi the unexpanded

unrotated Cartesian plane, and whose center is (u.v).

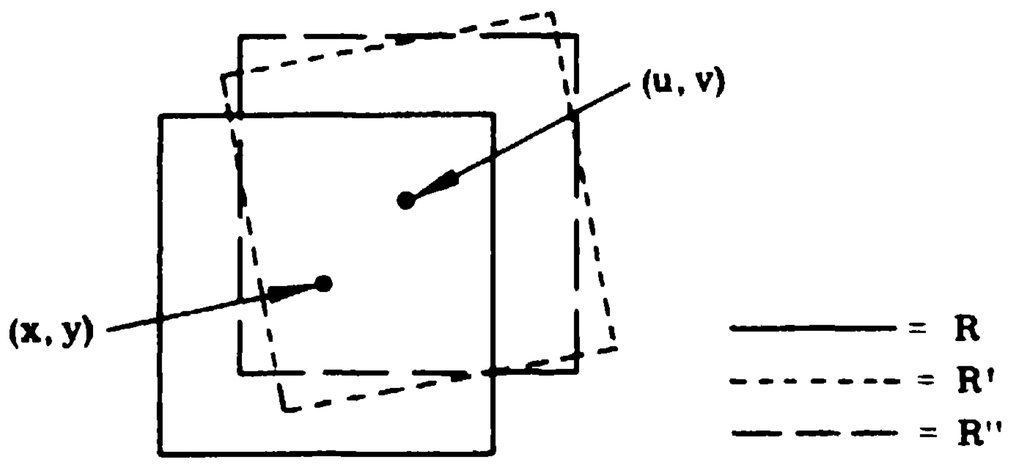

If θ is not far from 0 and α and β are close to 1, then the area of $R \cap R'$ is approximated by the area of $R \cap R''$

The distance between the left side of R and the left side of R'' is $|x - u|$. Consequently, it is not hard to see that the length of the bottom side of the rectangle $R \cap R''$ is $1 - |x - u|$, where $1 - a$ is defined as the maximum of the two numbers 0 and $1 - a$. Similarly, the other side of the rectangle $R \cap R''$ has length $1 - |y - v|$. Hence, the area of $R \cap R''$ is $(1 - |x - u|) \times (1 - |y - v|)$

Combining the above results, we determine that the area of $R \cap R'$ is approximated by

$$(1 - |x - \alpha x \cos\theta + \beta y \sin\theta|)$$

$$\times (1 - |y - \beta y \cos\theta - \alpha x \sin\theta|)$$

Thus,* $\phi_k = \phi(x, y) = (1 - f_1)(1 - f_2)$ where

$$f_1 = \min [|x - \alpha x \cos\theta + \beta y \sin\theta|, 1]$$

$$f_2 = \min [|y - \beta y \cos\theta - \alpha x \sin\theta|, 1]$$

and

θ = rotation angle
α = x scale factor
β = y scale factor

An Upper Bound on Sense Map Size

Based on the results ot the preceding section, it is possible to compute an upper limit on the size of a SM beyond which its area of overlap (with respect to resolution cells) with its original image in the RM ceases to increase. The entries in the following table give this limit as the dimension of one side of a square array of cells, as a function of rotation and uniform x,y scale factor.

*Note that if the map samples are not independent measurements, then the effective value of ϕ_k will be larger than the value given above. We are currently examining the heuristic of making ϕ_k an exponentially decreasing function of the distance between (x. y) and (u. v).

Scale Factor	Rotation (deg) 0	2	4	6
1.00	>50	>50	30	21
1.02	>50	>50	33	21
1.04	>50	>50	33	22
1.06	34	40	30	22
1.08	26	30	26	21
1.10	21	25	23	19

Note: (1) The values given in the above table are upper bounds rather than least upper bounds on map size.
(2) If the map samples are not independent measurements, then the table entries should be scaled upward. Thus, if sampling occurs at r times the Shannon rate, the table values can be r times their listed values.

Acknowledgment

The author would like to acknowledge the many technical contributions to this paper made by R. A. Elschlager. Thanks are also due to O. Firschein, J. M. Tannenbaum, and R. D. Merrill for helpful comments. The author's interest in the scene congruence problem was inspired by the work of W. G. Eppler [Ref. (13)].

Bibliography

(1) W. Miller and A Shaw, "Linguistic Methods in Picture Processing," AFIPS (FJCC) Proceedings, Vol 33. 1968. pp 279-290.
(2) M. A. Fischler. "The Detection of Scene Congruence," 6-83-71-2. Lockheed Palo Alto Research Laboratory, Jan 1971.
(3) T. W. Anderson, An Introduction to Multivariate Statistical Analysis, Wiley. 1958.
(4) A. Arcese, P H. Mengert, and E. W. Trombini, "Image Detection Through Bipolar Correlation," IEEE Trans, on Information Theory. IT-16(5), Sep 1970, pp. 534-541.
(5) C. K. Chow, "An Optimum Character Recognition System Using Decision Functions," IRE Trans, on Electronic Computers, EC-6. Dec 1957, pp. 247-254.
(6) P. W. Cooper, "The Hyperplane in Pattern Recognition," Cybernetica, Vol. 4. 1962.
(7) S. Goldman, Information Theory, Prentice-Hall, 1953.
(8) C. W. Helstrom, Statistical Theory of Signal Detection, Pergamon Press, 1960.
(9) N. J. Nilsson, Learning Machines, McGraw-Hill. 1965.
(10) G. S. Sebestyen, Decision-Making Processes in Pattern Recognition, Macmillan, 1962.
(11) J. M. Wozencraft and I. M. Jacobs, Principles of Communication Engineering, Wiley, 1965.
(12) W. B. Davenport, Jr., and W. L. Root, Random Signals and Noise, McGraw-Hill, 1958.
(13) W. G. Eppler and G. A. Simas, "A Theory of Map Matching," 5-26-68-2, Lockheed Missiles & Space Company, Mar 1968.